

Assisted Diagnosis System for Brain Diseases with Imbalanced Category Distribution Based on Medical Images

Junxiu Wang

Department of Computer Engineering, Taiyuan Institute of Technology, Taiyuan 030008, Shanxi, China
wangjx@tit.edu.cn

Abstract: The development of medical images has facilitated the diagnosis of brain diseases. The diagnosis of brain medical images has the characteristics of uneven distribution of categories and different costs of misclassification. Therefore, traditional classification algorithms are used in clinically confirmed MRI brains. When a medical image is used as a training set to construct a classification model, the classification effect is poor and it is easy to be insensitive to the positive class, which makes it difficult for the brain disease auxiliary diagnosis system to have high accuracy and weak generalization ability. The research purpose of this paper is to study the assistant diagnosis system of brain diseases based on the uneven distribution of medical image categories. In order to improve the performance of the assistant diagnosis system of brain diseases, this paper designs a cost-sensitive probabilistic neural network CS-PNN brain by introducing cost-sensitive this system is an auxiliary diagnosis system for diseases, and the reliability of the system is verified by experiments. It can be known from experiments that the cost-sensitive probabilistic neural network CS-PNN assisted diagnosis system for brain diseases designed in this paper increases with the cost of positive misclassifications and negative misclassifications, and the classification accuracy rate of CS-PNN continues to increase. $(01) = 4$ achieves the best classification performance of 97%. The research in this article provides new ideas for solving the problems of uneven distribution of categories and misclassification costs in MRI brain medical images, so as to develop a brain disease auxiliary diagnosis system with stronger generalization ability, thereby improving the diagnosis of brain tumors. Accuracy and reduce missed diagnosis.

Keywords: Medical Images, Imbalanced Distribution of Categories, Brain Diseases, Assisted Diagnosis Systems, Cost Sensitive

1. Introduction

The mutual penetration and development of clinical medicine and computer science have led to the increasing degree of automation of medical equipment. Computer-assisted brain tumor assisted diagnosis systems are the product of this development trend. If the patients can be more reliably identified before surgery, Symptoms to determine the type of tumor and the degree of deterioration will have a great impact on the formulation of a patient's treatment plan, thereby avoiding unnecessary surgical risks and expenses. With the continuous development of medical imaging technology and equipment, the use of CT, MRI and other medical images is increasing. At present, medical imaging data has become the largest source of data in hospitals. It usually can account for more than 80% of the data in a general hospital. They have become one of the most important decision-making basis for clinical diagnosis of doctors. The information of brain medical images has the characteristics of implicitness and ambiguity. At present, the diagnosis based on brain medical images is still mainly based on the doctor's naked eye for analysis. When the doctor performs naked eye analysis, it is not easy to find medical images. Many tiny texture changes in details and morphological characteristics, which affect the early judgment of the disease; when performing medical image diagnosis of the brain, it is easy to be limited by the doctor's business ability and mental state, fatigue and other subjective factors, and misdiagnosis, Missed diagnosis. Therefore, in the process of brain medical image diagnosis, doctors need to use computer-aided diagnosis system to improve the accuracy of diagnosis and reduce the rate of missed diagnosis.

The computer-aided diagnosis system can improve the accuracy of doctors' diagnosis, reduce the

workload, reduce the missed diagnosis and misdiagnosis caused by subjective factors such as the doctor's business ability and mental state, fatigue, and improve the difference between readers, but in the end The decision is still made by the doctor [1]. Therefore, the computer-aided diagnosis system should have similar abilities to doctors in learning and identifying brain diseases, and use image mining technology and machine learning technology to build computer-aided diagnosis systems, so as to improve the diagnosis ability of doctors. Brain medical image diagnosis usually has different characteristics of misclassification. The cost of misclassification in the diagnosis of brain diseases means that the cost of MRI brain medical images that originally belonged to the health category but were predicted to be cancerous is different from the cost that was originally predicted to be cancerous [2]. At this time, if the diagnosis system misdiagnoses the patient as health, it will delay the timely treatment of the patient, and even cause great harm to the patient's life and health; if the diagnosis system misdiagnoses the healthy person as the patient, although it will And medical staff bring some unnecessary trouble, but with further diagnosis and treatment, the misdiagnosis will be corrected, and the cost will be much smaller than the case of misdiagnosing the patient as healthy. Therefore, it is necessary to improve the generalization ability of the auxiliary diagnosis system and reduce the misdiagnosis rate of doctors' misdiagnosis of patients as health. It is a problem to be solved in the computer aided diagnosis system. The data involved in the diagnosis of brain medical images have the characteristics of uneven distribution of categories [3]. In the diagnosis of brain medical images, the imbalance of category distribution refers to the large difference in the number of sample sets between people with cancer and healthy people. For this case, traditional data mining techniques are used when the data distribution is unbalanced. The classification effect is poor, which makes it difficult for the auxiliary diagnosis system to have high accuracy [4]. Based on the above analysis, existing computer-aided diagnosis systems for brain diseases usually have shortcomings such as high feature vector dimensions, high computational complexity, and low generalization ability. This article studies brain disease mining algorithms based on the uneven distribution of categories of medical images. The design and implementation of an auxiliary diagnosis system is dedicated to improving the accuracy of doctors' diagnosis and reducing the rate of missed diagnosis. It has good application value and practical significance.

In the field of medical image processing, image segmentation plays an important role in extracting important and reliable features to determine tumor regions in magnetic resonance images. Among them, brain image segmentation is considered to be an interesting and difficult problem in this field. In order to improve the segmentation ability of fuzzy C-means algorithm and artificial bee colony algorithm (FCMABC), G Kagadis used the combination of fuzzy C-mean algorithm and artificial bee colony algorithm to extract the appropriate number of cluster centers (tumor areas). G Kagadis proposed A new automatic intelligent clustering method for segmenting brain tumors uses an automatic and dynamic approach to the number of abnormal cells in each cluster (multiple sclerosis). G Kagadis compared the algorithm with the traditional FCM algorithm. The experimental results of G Kagadis show that FCMABC proposed by G Kagadis is effective in improving the accuracy of traditional FCM clustering. Compared with traditional FCM, the algorithm has stronger robustness and anti-noise ability [5-6]. Medical image processing plays an important role in supporting the diagnosis of various diseases. Brain magnetic resonance imaging (MRI) images are widely used to support doctors' decisions, and doctors will decide if there are any problems in the brain. The essence of MRI is segmentation, which is the basis for the selection of the damaged area, quantitative measurement and three-dimensional reconstruction. In order to effectively identify positioning targets, Snehashis Roy once proposed a segmentation algorithm based on global entropy minimization. The algorithm uses a secondary segmentation method based on the clustered area image model to overcome the negative effects of shift segmentation. The experimental results of Snehashis Roy show that the algorithm has the best performance and highest accuracy. In terms of similarity, the performance of this algorithm is almost the same as that of Least Deviation Fuzzy Clustering Algorithm (LBFC), and its performance is 10% higher than that of Fuzzy C-Means Clustering Algorithm (FCMA) [7-8]. Mutasem K. Alsmadi has applied the RBF group method of data processing (GMDH) neural networks to medical image analysis of magnetic resonance imaging (MRI) brain images. In this deep RBF GMDH-type neural network algorithm, Mutasem K. Alsmadi uses the basic premise of the GDH algorithm-a heuristic self-organizing method, to automatically generate and organize multiple hidden layers to adapt to the complexity of nonlinear systems. This heuristic self-organizing method is an evolutionary computation. Mutasem K. Alsmadi applies deep RBF-GMDH neural network to medical image analysis of MRI brain images, and uses deep-RBF-GMDH neural network to accurately identify and extract white and gray matter regions of the brain. These recognition results are compared with the recognition results of a traditional sigmoid sinus function neural network trained with the back-propagation method [9-10].

The innovation of this paper is that by introducing a cost-sensitive mechanism, a traditional cost-insensitive probability neural network based on density function kernel estimation is designed as a cost-sensitive probabilistic neural network CS-PNN to solve the uneven distribution of categories in MRI brain medical images. And misclassification costs, so as to develop a brain disease assistant diagnosis system with stronger generalization ability, in order to improve the accuracy of brain tumor diagnosis and reduce the rate of missed diagnosis.

2. Proposed Method

2.1 Commonly Used Medical Image Denoising Methods

The medical images obtained by digital medical imaging equipment are mainly affected by pulse noise, salt and pepper noise, and Gaussian noise. Because the noise reduces the image quality, it cannot meet the doctor's requirements for image vision, which prevents the visual organs from understanding that at the same time, it will also have a direct impact on image segmentation, feature extraction, and construction of classification models during medical image analysis [11]. Therefore, the presence of noise in medical images seriously interferes with the identification and analysis of medical images. Medical images collected in real time must be denoised before image processing such as image segmentation and feature extraction. Denoising processing is to ensure high accuracy in subsequent operations. One of the steps is to eliminate the noise components in the medical image to make the image clearer, the visual effect is better, and the useful information carried by the medical image is not lost [12]. Due to the presence of noise in medical images, doctors cannot accurately detect the lesion area, and for computer-assisted diagnostic systems, even a small amount of noise can change the classification results. Therefore, the medical image needs to be denoised to improve the medical image. Quality [13-14]. According to different denoising algorithms to reduce the noise in medical images, commonly used medical image denoising methods can be divided into pixel domain method and frequency domain method. The pixel domain method is also called the spatial domain method. The pixel domain method is to perform some calculation on a pixel in the image and all elements in the neighborhood of the pixel, and use the calculation result to replace the pixel value in the original image. The pixel value of is directly related to the elements in the neighborhood. Therefore, the pixel domain method is an image-based neighborhood processing method. From the perspective of geometry, it can be divided into linear filtering method and nonlinear filtering method. The frequency domain denoising method is to use a function to transform the image from the spatial domain to the frequency domain, and then inverse transform the transformed frequency domain spatial image to obtain a clear image after denoising [15-16].

(1) Linear filtering

1) Gabor filtering

Gabor filtering, while reducing image noise, can retain important information required for subsequent image processing. It is a linear filter for edge detection. The frequency and direction expression of Gabor filtering is similar to the human visual system, and is especially suitable for texture discrimination and analysis. The advantages of Gabor filtering in image denoising are uniqueness, specificity to a certain period and scale, fast Fourier analysis using FFT, and correlation with quantitative signals; the disadvantage is that the size of the image required by FFT is about 2 (= 012), there is a boundary condition problem, and the time and frequency domain descriptions of the signals are opposite.

2) Adaptive filtering

Adaptive filtering does not have any impact on the original image while reducing the impulse noise on the image. It is used to eliminate the unknown interference contained in the main signal. The main signal is used for the expected response of the adaptive filter. The reference signal is used as the input of the filter. Adaptive filtering has two advantages when performing image denoising processing: first, it can reduce smooth and non-rejective noise, but the edges of the image will not become blurred; second, it can retain edge information in the case of high-density impulse noise; the disadvantage is that When the impulse noise is greater than 0.2, the denoising performance is not good.

3) Mean filtering

The main idea of mean filtering is to add the neighborhood pixel values of each pixel in the image, then find the average value of these pixels, and use the average value to replace the pixel value of the

pixel point in the original image. It can eliminate the non-representation Pixels. Mean filtering is generally considered as a type of convolution filter. It is a convolution operation based on a convolution kernel. The convolution kernel represents the shape and size of the neighborhood to be sampled when calculating the average. Using a 3×3 square kernel, You can also use a larger kernel for smoothing. The advantages of mean filtering when performing image denoising processing are that it can reduce the difference and is easy to perform; there are three disadvantages: one is that the smoothing operation will cause the edge of the image to become blurred while affecting the localization of the image while denoising, and the other is the pulse Noise has not been completely eliminated. Third, it will affect the average value of all pixels in the neighborhood.

4) Wiener filtering

Wiener filter is a linear filter that has been widely used to restore images with noise and blur. The important use of Wiener filter is to reduce the noise in the image by comparing it with the desired noise-free signal. It is A statistical-based method. The advantage of Wiener filtering in image denoising is that minimizing the mean square error is an effective work and can deal with the degradation function and noise; the disadvantage is that the reasonable estimation efficiency of the degradation function is low.

(2) Non-linear filtering

Non-linear filtering methods cannot be expressed by linear mathematical expressions. They are discontinuous and discontinuous. Typical techniques include morphological operations and histogram equalization.

1) Morphological operation

The morphological operation uses a small template of structural elements to detect the image. The structural elements are located in all possible positions of the image. The selected structural elements are compared with the corresponding pixel neighborhood. Erosion and dilation are two basic morphological operations, where erosion removes the boundary points smaller than the structural elements from the binary image, but at the same time reduces the size of the region of interest; the dilation operation usually uses structured elements to detect and expand the input image. shape. In compound operations, many morphological operations are a combination of erosion, expansion, and simple set theory operations, such as the addition of binary images. The opening operation first performs erosion, and then swells the results after erosion, and expansion is more destructive than erosion. Small; closed operation first performs expansion, and then erodes the result of the expansion. The closed operation is because it can fill the holes in the area while maintaining the size of the initial area. The advantage of morphological operation in image denoising is that it can detect lesions of various sizes and shapes, including complex shapes; the disadvantage is that the morphological operation relies on the concept of upper and lower limits.

2) Histogram equalization

Histogram equalization is a traditional method for removing background. As mentioned earlier, the dilation operation usually uses structured elements to detect and expand the shape of the input image. This method usually increases the overall contrast of the image, especially when the effective data of the image is represented by approximate contrast values, and the histogram is equalized. Use the image histogram to adjust the contrast. The intensity of the image can be better distributed on the histogram, allowing lower local contrast areas to obtain higher contrast. Histogram equalization achieves this by effectively dispersing the most frequent intensity values. For one thing, this method is useful in images where both the background and foreground are bright or both are dark. The advantages of histogram equalization in image denoising are simple and can enhance the contrast of the image; the disadvantage is that if there are gray values in the image that are physically far away from each other, this method will fail.

2.2 DICOM Medical Image Standard

(1) Overview of DICOM Standard

Different storage methods and different operation interfaces of different manufacturers' equipment have brought some problems to the clinic. In order to solve this problem, scholars combined the relevant technical information used worldwide to formulate the DICOM standard, which provides two standards for medical imaging imaging technology standards and transmission communication

technology standards [17]. The standard almost covers today's mainstream information and communication protocols. It uses an object-oriented method to specify a complete set of commands for medical images from acquisition and analysis to report diagnosis. It has developed a unique DICOM file format for image files, identified unique identifiers, and provided The docking of the backbone Internet has greatly promoted the development of medical imaging with openness and interconnection, and laid the foundation of the remote consultation system [18-19].

(2) DICOM file format

1) The basic structure of DICOM files

The DICOM file format is a multi-layered file format based on the DICOM standard. It has a clear structure and clear data elements. Generally, it consists of two major structures: file header and data set [20]. The first layer of the file layer, the file layer contains all the basic information of the file in the DICOM file format, is a necessary content in the entire file, including the preface of the file and the general information header of the file. The file layer can perform the operation response to the most basic functions such as opening, closing, and browsing of files. It supports the browsing and viewing of file attributes and transmission paths, and the browsing and printing of file contents. It is an integral part of the entire file [21]. The second layer is the data set layer. As the name suggests, a data set is a collection of data elements [22]. The data set layer contains data sets composed of different module information. The information carried in these data sets reflects the image content well. The content of each information module can be operated on the data set layer. The third layer is the module layer. The module layer rearranges and combines file information in a class manner. Regrouping the information of the same category in different groups together helps to quickly retrieve the required content and facilitates the operation of the module in the data set. The fourth layer is the element layer. The element layer is the most basic layer of a DICOM file. Each element in the element layer is the smallest entity in the entire file format.

2) Data elements of DICOM files

Data element is the smallest entity unit in the entire DICOM file. It is mainly divided into four parts: label, data description, data length and data field. The tag of the data element is used to identify the type of the element, and it is the ID of the data element. Can be divided into standard data elements and private data elements by identification tags [23]. As the unique identification mark of the data element, the label can not be repeatedly defined and used. Data description is simply a string describing the type of data. The contents of the character string can clearly reflect the characteristics of the data element [24-25]. The data length is an even number to represent the number of bytes of information contained in the data element. When the number of bytes is odd, it is complemented by the "+1" algorithm. The data length specific indicates that the data field is worth the length. The value range represents the data conclusions obtained by the algorithm from all the content in the definition field of the data element, and reflects the actual value of the data element. The data can be calculated by the way of data elements. Countless data elements are brought together in a certain arrangement to form a data set. The data set and DICOM file header are combined to form a standard DICOM file. The DICOM standard stipulates that the data elements of the file are allowed to be customized, so that the DICOM file contains the necessary medical image information, as well as information on each step in the entire examination process with the patient, from the patient's personal information to the collection Data parameters can constitute data elements recorded in DICOM files. This enables a complete DICOM file to have complete medical information functions, avoiding the possibility of data inaccuracy and loss in the information interactive transmission of various systems. Using specific professional software to open the DICOM file, you can view the complete patient information. This design greatly facilitates the clinician to view the patient's related information during the consultation, and also facilitates the inspection technician to check the patient's previous medical history, reducing the risk of diagnosis and treatment. At the same time, the system only needs a simple data interface to achieve good compatibility.

2.3 Cost-Sensitive Learning

The traditional classification algorithms all aim at minimizing the classification error rate, and assume that the training data sets of various types are balanced, and the cost of misclassification is equal. It is not balanced and the cost of misclassification is also unequal. Traditional classification algorithms will get a lower classification error rate but this classification model is meaningless. Cost-sensitive learning assigns different costs to different misclassifications by introducing

cost-sensitive factors, so that traditional classification algorithms can meet the needs of medical image diagnosis to a certain extent.

Cost-sensitive learning can be divided into two categories:

(1) It operates at the data level, and operates the training set through the cost matrix and changes its distribution, so that the traditional classification algorithm is effective. , Oversampling, and resampling, but these methods have some disadvantages:

- 1) Operating on the training set will lose some useful information.
- 2) Prone to overfitting,
- 3) The best classification model for a training dataset is usually unknown,
- 4) In most cases, the extra learning cost of analyzing and processing the training data set is inevitable;

(2) Operate the classification algorithm, keep the training data set unchanged, and design a cost-insensitive classification algorithm into a cost-sensitive classification algorithm by introducing a cost-sensitive factor, so-called cost-sensitive direct learning. For cost-sensitive direct learning, different misclassifications have different costs. When a positive error is classified as a negative class, a higher misclassification cost is assigned, and when a negative error is classified as a positive class, a lower misclassification cost is assigned. Strategies to solve the problem of uneven distribution of categories, thereby improving the recognition of positive categories.

Through cost-sensitive direct learning, a clinically diagnosed MRI brain medical image with an uneven distribution of categories is used as a training set to build a classification model, and this classification model is used to classify MRI brain medical images into normal and abnormal (i.e., brain tumor patients) Two categories.

When processing MRI brain medical images with uneven distribution of categories, the cost of misclassification is higher than the cost of correct classification, that is, $C(1,0) > C(0,0)$ and $C(0,1) > C(1,1)$; positive examples are more important than negative examples. Therefore, it is more costly to misclassify patients who are actually cancerous as normal than to be cancerous, which is that the CFN value is greater than the CFP value, or $C(0,1) > C(1,0)$; when MRI brain medical images are correctly predicted The cost of misclassification is 0, that is, $CTN = CTP = 0$ or $C(0,0) = C(1,1) = 0$. Cost-sensitive learning attempts to minimize the error rate of high-cost samples and minimize the total cost of misclassification. Cost-sensitive classification algorithms will consider the cost matrix when building a classification model and generate the classification model with the lowest misclassification cost.

Given the misclassification cost matrix, an instance should be predicted as the one with the lowest expected cost, that is, the principle of the lowest expected cost is followed. The expected cost $R(i|x)$ of classifying the prediction sample X into the i class is defined as:

$$R(i|x) = \sum_j C(i, j)P(j|x) \quad (1)$$

According to the principle of minimum expected cost, a cost-sensitive classifier to classify MRI brain medical images as positive needs to satisfy the following formula:

$$(C(1,0) - C(0,0))P(0|x) \leq (C(0,1) - C(1,1))P(1|x) \quad (2)$$

When the MRI brain image is correctly predicted, its misclassification cost is zero, and the above formula can be transformed into the following formula:

$$C(1,0)P(0|x) \leq C(0,1)P(1|x) \quad (3)$$

2.4 Cost-Sensitive Probabilistic Neural Networks with Imbalanced Class Distribution of Brain Images

(1) Classification performance evaluation based on imbalanced category distribution

The evaluation index plays a crucial role in classifier performance evaluation and guidance of classifier modeling. The cost-insensitive classification algorithm is designed based on maximizing classification accuracy. At this time, accuracy is the most commonly used performance evaluation index. However, for the classification of brain medical images with unevenly distributed categories, the

classification accuracy is no longer suitable as an evaluation criterion, because the number of negative samples in the training samples of MRI brain medical images is much larger than the number of positive samples. At this time, the classifier will give more weight to the negative class for accuracy, and the positive class will have less influence on the accuracy than the negative class. For example, the samples of the positive category account for 1% of the training sample set, and the samples of the negative category account for 99% of the training sample set. Using the sample set with uneven distribution in this category to build a classification model, the accuracy of the classifier can reach 99%. However, this performance evaluation is not suitable for brain medical image diagnosis, because we pay more attention to the recognition rate of positive classes. The classification model is constructed using MRI medical images of imbalanced category distribution as the training set. The receiver operation characteristic curve, AUC, F-measure, G-mean and other indicators are used to evaluate the performance of the classifier. These indicators are based on the confusion matrix. Assessed.

(2) Cost-sensitive probability neural network

In this paper, by introducing a cost-sensitive mechanism, a traditional cost-insensitive probability neural network based on density function kernel estimation is designed as a cost-sensitive probabilistic neural network, which solves the problems of uneven class distribution and misclassification cost in MRI brain medical images. In this paper, clinically diagnosed MRI brain medical images with uneven distribution of categories are used as a training set, and a cost-sensitive probabilistic neural network proposed in this paper is used to build a classification model for this training set. The classification model is used to classify MRI brains of unknown categories. Medical images are classified into normal (that is, healthy) or abnormal (that is, suffering from cancer), so as to minimize the total misclassification cost and improve the generalization ability of the classification model while ensuring a certain classification accuracy.

(3) Network model of cost-sensitive probabilistic neural network

The cost-sensitive probabilistic neural network CS-PNN is based on the theory of minimum risk Bayesian decision and the mixed Gaussian density function in Parzen window method. , Gaussian mixture layer, cost mechanism introduction layer and output layer. The functions of each layer are as follows.

1) Input layer

The test sample $X = (x_1, x_2, \dots, x_7)$ is the feature vector selected by the PCA from the wavelet coefficients, that is, the dimension of the input sample is 7, so the input layer is composed of 7 neurons. Incoming network. The function of the input layer of the CS-PNN is the same as that of the input layer of the probability neural network based on the density function kernel estimation. The input and output of the i neuron in the input layer are X_i and Y_i , respectively.

$$X = (x_1, x_2, x_3, x_4, x_5, x_6, x_7), YI_k = X_k, k = 1, 2, \dots, 7 \quad (4)$$

2) Mode layer

The number of neurons in the mode layer is equal to 188, because 188 clinically diagnosed MRI brain medical images are used as training samples, of which 180 are MRI brain medical images of healthy people and 8 are MRI brain tumor images. Each neuron in the pattern layer corresponds to an MRI brain image in a training sample and is used to receive a feature vector selected by the PCA from the wavelet coefficients, because the feature vector represents the original MRI brain image. The function of the pattern layer is to calculate the distance between the feature vector of the test sample and each training sample in the training set. The feature vector here refers to the feature vector selected by PCA from the wavelet coefficients, which reflects the MRI brain image of the test sample and the training set. The matching degree or similarity of each MRI brain image, and then the non-linear mapping of the distance is performed by the normalized Gaussian kernel function to obtain the output YM_i of the pattern layer.

$$YM_{ij} = p_{ij}(x) = \exp\left(-\frac{(x - x_{ij})(x - x_{ij})^T}{2\sigma^2}\right) = \exp\left(\frac{x^T x_{ij} - 1}{\sigma^2}\right) \quad (5)$$

3) Gaussian mixing layer

The number of neurons in the Gaussian mixture layer is equal to the number of categories, that is, equal to two, and it is connected to the mode layer through the mixed Gaussian density function. The

function of the Gaussian mixture layer is to calculate the probability density function $g_i(x)$ of the test sample $X = (x_1, x_2 \dots x_7)$ under various conditions.

$$g_i(x) = YH_{ij} = \sum_{j=1}^{G_i} \pi_{ij} p_{ij}(x), i = 2 \quad (6)$$

4) Cost mechanism introduction layer

The number of neurons in the cost mechanism introduction layer is equal to the number of categories in the training set. Because there are two types of MRI brain medical images, that is, normal or abnormal (negative or positive), the number of neurons in the cost mechanism introduction layer is 2, each Each neuron corresponds to a category. In the diagnosis of brain medical images, because different misclassifications will cause different degrees of loss, it is better to expand some total error rates and reduce the total loss. The expected loss $R(\alpha_N|x)$ of the test sample $X = (x_1, x_2 \dots x_7)$ under the condition of the cost function is defined as:

$$R(\alpha_N|x) = \sum_{i=1}^c Cost(\alpha_N|\omega_i) * g_i(x) * p(\omega_i) \quad (7)$$

5) Output layer

The number of neurons in the output layer is 1. The output layer is also called the decision layer. It has a decision function. It uses the minimum risk Bayesian decision as the theoretical basis to make a decision on the category to which the test sample $X = (x_1, x_2 \dots x_7)$ belongs.

$$Class(X) = \arg \min R(\alpha_N|x), N = 2 \quad (8)$$

3. Experiments

3.1 Automatic Segmentation Experiments of Brain Images

The pulse coupled neural network and Markov random field model were used to segment MRI brain medical images of 40 patients with tumors. The segmented MRI brain medical images were used in the process of identifying the region of interest (TheRegionOfInterest, ROI). C-ROI, P-ROI and N-ROI for performance evaluation, where C-ROI indicates that the ROI in the MRI brain medical image was correctly identified by PCNN and MRF, and P-ROI indicates that part of the ROI in the MRI brain medical image was identified by the PCNN and MRF identified it, and N-ROI indicates that no ROI in the MRI brain medical image was correctly identified by PCNN and MRF.

3.2 Experimental Design

(1) Experimental environment

The environment configuration of this paper is shown in Table 1. The SQL Server database is used to store the wavelet coefficients extracted from MRI brain medical images by DWT and the PCA feature vector after wavelet coefficient reduction.

Table 1: Configuration of experimental environment

Type	Configure
CPU	AMD FX(tm)-8150Eight-Core Processor
Internal storage	16G
Operating system	Windows 10
Disc	1T
Data base	SQL Server
Matlab	3.5

(2) Experimental data set

Using 240 MRI brain medical images as the experimental data set, 200 of which are normal and 40 abnormal (brain tumor patients), these datasets are composed of axial, T2-weighted, 256 * 256 pixels MRI brain medical images, From the TCIA Cancer Medical Image Management Website. The experiment uses a ten-fold cross-validation method. Each experiment randomly selects 180 samples from 200 normal samples, and at the same time randomly selects 18 samples from the 40 abnormal samples as the training set, and the remaining 22 samples as the test set. To verify the performance of

the classification model constructed by cost-sensitive probabilistic neural networks on these imbalanced datasets.

(3) Misclassification cost setting

In the experiment, when the correct prediction is made, the cost of misclassification is 0, that is, $Cost(0,0) = Cost(1,1) = 0$; the actual misdiagnosis of patients with cancer is normal than the normal misnomer. Dividing into cancer has a higher cost, that is, $Cost(0,1) > Cost(1,0)$. However, the specific values of $Cost(01)$ and $Cost(10)$ cannot be obtained from the data set of this experiment. Therefore, the value of $Cost(10)$ is fixed to be equal to 1 in the experiment, and the value of $Cost(01)$ is changed by changing the value. The misclassification cost function is defined as:

$$Cost[i, j] = \begin{cases} 0, & i = j \\ c_n, i > j, & i, j = 0,1 \\ ikc_n, k = [1,6], \text{ And } i < j \end{cases} \quad (9)$$

The cost matrix applied to the experiment is shown in Table 2.

Table 2: Misclassification cost matrix for brain image diagnosis

	Cost(0,0)	Cost(0,1)	Cost(1,0)	Cost(1,1)
0	0	0	0	0
1	0	1	1	0
2	0	2	1	0
3	0	3	1	0
4	0	4	1	0
5	0	5	1	0
6	0	6	1	0

As can be seen from Table 2, when $Cost(0,0) = Cost(1,1) = Cost(0,1) = Cost(1,0) = 0$, it means that the cost of misclassification is not considered, that is, the CS-PNN is degraded to ME-PNN; in the case of 0-1 cost function, that is, $Cost(0,0) = Cost(1,1) = 0$ and $Cost(0,1) = Cost(1,0) = 1$, at this time The decision result of CS-PNN is the same as the decision result of ME-PNN. CS-PNN also degenerates to ME-PNN.

4. Discussion

4.1 MRI Brain Image Segmentation Based on PCNN

PCNN based on biological model is a single-layer neural network, which can realize MRI brain medical image segmentation without training. When PCNN performs segmentation processing on MRI brain medical images, the number of neurons is equal to the number of pixels of the input MRI brain medical images. Each pixel in the image is connected to a unique neuron, and each neuron passes The radius of the connection domain is connected to surrounding neurons. The effect of before and after segmentation processing of MRI brain medical images using pulse coupled neural network PCNN is shown in Figure 1.

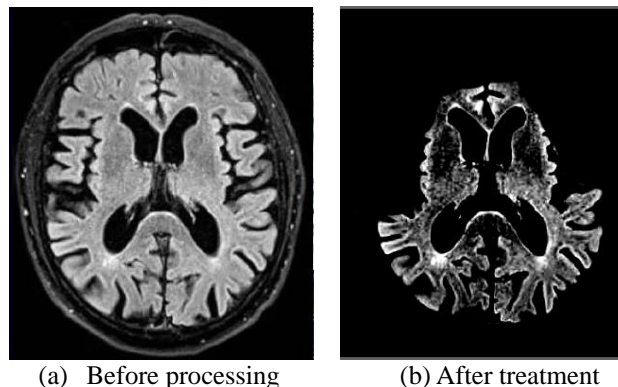


Figure 1: Effect map of MRI brain medical image before and after segmentation by PCNN

From Figure 1, we can see the effect of before and after segmentation processing of MRI brain

medical images using the pulse coupled neural network PCNN. In the case of selecting PCNN parameters, it is also important to determine the optimal number of iterations for the segmentation processing of MRI brain medical images by PCNN, because the number of iterations will directly affect the processing speed and segmentation effect of PCNN. In this paper, the maximum information entropy criterion is used to determine the optimal number of iterations for segmentation, so as to achieve the purpose of automatic segmentation. The specific method is to calculate the information entropy of the segmented image output at each iteration under the condition of setting the number of iterations N. The segmented image with the maximum information entropy in N iterations is the one with the best selection under the selected parameter model. The number of iterations is the optimal number of iterations for the segmented image of the segmentation effect. Through a large number of experiments, it was found that when the PCNN performs MRI brain medical image segmentation, the image can obtain the maximum information entropy within 15 iterations, and segment the image to achieve the best results, so in this article, the number of iterations $N = 15$, which reduces At the same time, the processing speed of the PCNN is increased.

4.2 Experimental Results and Analysis

(1) Classification performance analysis

This paper uses cost-sensitive probabilistic neural networks, Bayesian decision rules based on minimum error rate, probabilistic neural networks, cost-sensitive decision trees, and cost-sensitive BP neural networks to classify MRI brain medical image data sets with uneven class distribution. The classification cost matrix is shown in Table 3.

Table 3: Misclassification cost matrix

	It actually negative	Is actually positive
The prediction is negative	Cost(0,0)	Cost(0,1)
The prediction is positive	Cost(1,0)	Cost(1,1)

As can be seen in Table 3, 0 indicates negative, 1 indicates positive, and Cost () indicates the misclassification cost of predicting the MRI brain medical images that actually belong to the class as class i. In the diagnosis of brain medical images, when the correct prediction is made, the cost of misclassification is 0, that is, $Cost(0,0) = Cost(1,1) = 0$; the patients who actually have cancer are mistakenly divided into normal ratios. Actually, the normal misclassification of cancer has a higher cost, so $Cost(0,1) > Cost(1,0)$. In the misclassified cost matrix, the cost function $Cost(0,0) = Cost(1,1) = 0$. When the cost function $Cost(0,1) = Cost(1,0) = 0$, it indicates that the negative error is classified as The cost of categorizing masculine and feminine errors into negatives is zero. At this time, CS-PNN is a probabilistic neural network based on the Bayesian decision rule with the minimum error rate; When $N = 123$, it means that the cost of negative misclassification is equal to the cost of negative misclassification, that is, in the case of a 0-N cost function, the decision result of the cost-sensitive probability neural network is based on the minimum error rate. The decision result of the probabilistic neural network based on the decision rule of CS, at this time CS-PNN is equivalent to ME-PNN. Therefore, the cost-sensitive probabilistic neural network proposed in this paper has stronger generalization ability than traditional probabilistic neural networks.

The classification performance of CS-PNN and ME-PNN is shown in Figure 2.

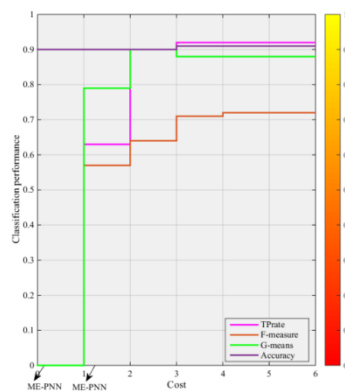


Figure 2: Classification performance of CS-PNN and ME-PNN

It can be seen from Figure 2 that when the cost of misclassification is zero, the correct classification accuracy of ME-PNN for positives is zero, that is, the sensitivity of positives is 0; when $\text{Cost}(0, 1) \geq 3$, CS-PNN can obtain the best The recall rate of = 1 is much higher than the recall rate of ME-PNN. As the cost of misclassification of positives and negatives continues to increase, the classification accuracy rate of CS-PNN continues to increase. When $\text{Cost}(0,1) = 4$, the best classification performance reaches 97%. F-measure and G-means continue to increase as the cost of positive misclassifications of negative misclassifications changes. When $\text{Cost}(0,1) = 2$, G-means quickly reaches the optimal value of 0.93. When $\text{Cost}(0,1) \geq 4$, F-measure, G-means, and accuracy no longer change and reach their peaks.

(2) Analysis of positive sensitivity

The clinically diagnosed 188 cases of MRI brain medical images with unevenly distributed categories are used as a training set. A cost-sensitive probabilistic neural network is used to build a classification model for this training set. The classification model is used to classify MRI brain medical images of unknown categories as Normal (ie healthy) or abnormal (ie cancer). The sensitivity of CS-PNN, CS-BPNN and CS-Tree to positive is shown in Figure 3.

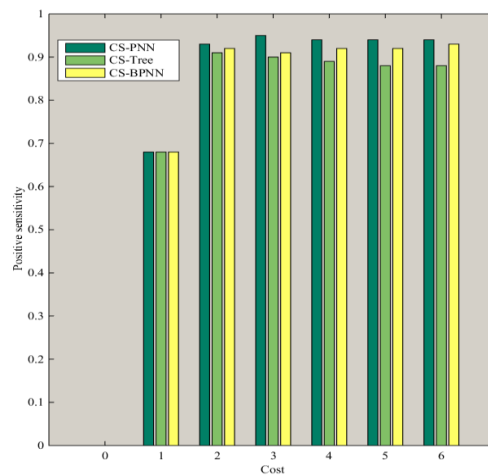


Figure 3: Analysis of cs-pnn, cs-bpnn and CS tree for positive sensitivity

As can be seen from Figure 3, as the cost of misclassification of positive misclassifications into negatives continues to increase, CS-PNN is particularly sensitive to positives and can quickly reach the optimal state of positive sensitivity1; CS-Tree is less costly for misclassification Sensitivity, its positive sensitivity will no longer change when it reaches a certain state; CS-BPNN changes slowly to positive sensitivity and cannot reach the optimal state quickly.

(3) Analysis of the average result of cross-validation of 10% off the modeling time

The average result of ten-fold cross-validation of modeling time is shown in Figure 4.

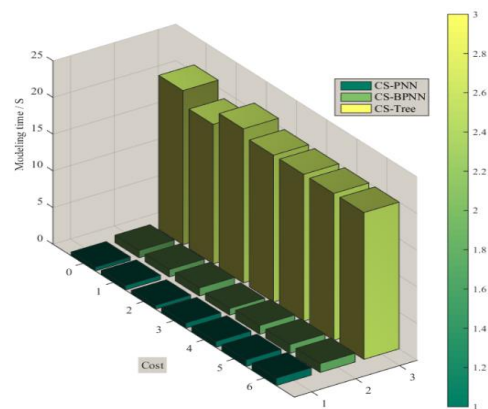


Figure 4: Comparative analysis of modeling time of cs-pnn, cs-bpnn and CS tree

From Figure 4, it can be seen that the modeling time of CS-PNN is about 1/4 of CS-Tree, and the modeling time of CS-PNN is about 1/22 of CS-BPNN. related. For computer-aided diagnosis system, modeling time is extremely important, so it must meet the real-time requirements. Among the three cost-sensitive algorithms, CS-PNN, CS-BPNN and CS-Tree, the real-time performance of CS-PNN is better.

(4) System accuracy analysis

When Cost (0,1) = 4, the ROC curves of CS-PNN, CS-BPNN and CS-Tree are shown in Figure 5.

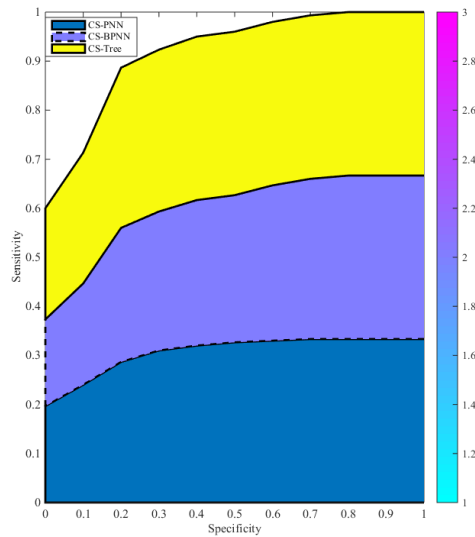


Figure 5: ROC curve

As can be seen from Figure 5, the area under the ROC curve corresponding to CS-PNN is larger than the area under the ROC curve corresponding to CS-BPNN and CS-Tree, where the AUC of CS-PNN = 0.98, so the medical image-based category developed in this paper The unevenly distributed brain disease diagnosis system has high accuracy.

5. Conclusions

Brain medical image diagnosis has the characteristics of uneven class distribution and misclassification costs. Traditional classification algorithms have poor classification results and are easy to be insensitive to positive classes. As a result, it is difficult for the auxiliary diagnosis system for brain diseases to have high accuracy. And the generalization ability is weak. Aiming at the shortcomings of traditional classification algorithms, this paper introduces a cost-sensitive mechanism to design a traditional cost-insensitive probability neural network based on density function kernel estimation into a cost-sensitive probabilistic neural network CS-PNN to solve MRI brain medical images. Classes are unevenly distributed and misclassified at different costs.

The cost-sensitive probabilistic neural network CS-PNN proposed in this paper constructs a classification model for this training set, and uses this classification model to classify MRI brain medical images of unknown categories into normal (ie, healthy) or abnormal (ie, cancer). Through experimental verification, it can be seen that the cost-sensitive probabilistic neural network algorithm proposed in this paper reduces the total misclassification cost while ensuring classification accuracy, and has stronger generalization ability than traditional classification algorithms.

This paper implements two modules of constructing classification model and performance evaluation in CIBMICAD auxiliary diagnosis system. Based on the imbalanced MRI brain medical image data set, the classification performance evaluation indicators with imbalanced class distribution and the use of cost-sensitive BP neural network and cost-sensitive decision tree are compared with price-sensitive probabilistic neural network to verify the proposed in this paper. The effectiveness of cost-sensitive probabilistic neural network CS-PNN algorithm.

References

- [1] Teitelbaum, Gillian A, Teitelbaum, Jonathan E. Uneven Distribution of Microgranules in Divided Lansoprazole Tablets [J]. *Journal of Pediatric Gastroenterology & Nutrition*, 2015, 61(4):437-9.
- [2] Yipeng Liu, Chaoqing Xu, Zhechen Jiang. A Survey on Brain Fiber Visualization [J]. *Jisuanji Fuzhu Sheji Yu Tuxingxue Xuebao/Journal of Computer-Aided Design and Computer Graphics*, 2018, 30(1):9.
- [3] Yang, Haiwei, Wang, Fei, Jiang, Peilin. Accurate Anatomical Landmark Detection Based on Importance Sampling for Infant Brain MR Images [J]. *Journal of Medical Imaging & Health Informatics*, 2017, 7(5):1078-1086.
- [4] Zhang, Xiyu, Liu, Xinqi, Lin, Weiwei. Computing Optimization Technique in Enhancing Magnetic Resonance Imaging and Brain Segmentation of Hypophysis Cerebri Based on Morphological Based Image Processing [J]. *Journal of Medical Imaging & Health Informatics*, 2016, 6(4):1063-1070.
- [5] G Kagadis, C Alexakos, P Papadimitroulas. SU-E-I-69: A Cloud Based Application for MRI Brain Image Processing [J]. *Medical Physics*, 2015, 42(6):3257.
- [6] Biswajit Biswas, Biplab Kanti Sen. Color PET-MRI Medical Image Fusion Combining Matching Regional Spectrum in Shearlet Domain [J]. *International Journal of Image and Graphics*, 2019, 19(1):1950004.
- [7] Snehashis Roy, Qing He, Elizabeth Sweeney. Subject Specific Sparse Dictionary Learning for Atlas Based Brain MRI Segmentation [J]. *IEEE Journal of Biomedical & Health Informatics*, 2015, 19(5):1598.
- [8] Subhranil Koley, Ashwini Galande, Bhooshan Kelkar. Multispectral MRI Image Fusion for Enhanced Visualization of Meningioma Brain Tumors and Edema Using Contourlet Transform and Fuzzy Statistics: [J]. *Journal of Medical & Biological Engineering*, 2016, 36(4):1-15.
- [9] Mutasem K. Alsmadi. MRI Brain Segmentation Using a Hybrid Artificial Bee Colony Algorithm with Fuzzy-C Mean Algorithm [J]. *Journal of Applied Sciences*, 2015, 15(1):100-109.
- [10] Yuanpeng Zhang, Li Wang, Huiqun Wu. A Clustering Method Based on Fast Exemplar Finding and Its Application on Brain Magnetic Resonance Images Segmentation [J]. *Journal of Medical Imaging & Health Informatics*, 2016, 6(5):1337-1344.
- [11] Pan, Xiang, Liu, Shuangshuang, Jiang, Taiping. Non-Causal Fractional Low-Pass Filter Based Medical Image Denoising [J]. *Journal of Medical Imaging & Health Informatics*, 2016, 6(7):1799-1806.
- [12] Hilal Naimi, Amel Baha Houada Adamou-Mitiche, Lahcène Mitiche. Medical image denoising using Dual Tree Complex Thresholding Wavelet Transform and Wiener filter [J]. *Journal of King Saud University - Computer and Information Sciences*, 2015, 27(1):40-45.
- [13] Mostafa Heydari, Mohammad Reza Karami. A New Adaptive Diffusive Function for Magnetic Resonance Imaging Denoising Based on Pixel Similarity [J]. *Journal of Medical Signals & Sensors*, 2015, 5(4):201-209.
- [14] Shuo Yang, Jianxun Li. The Design of Composite Adaptive Morphological Filter and Applications to Rician Noise Reduction in MR Images [J]. *International Journal of Imaging Systems & Technology*, 2015, 25(1):15-23.
- [15] Wei Zhao, Tianye Niu, Lei Xing. MO-FG-204-03: Using Edge-Preserving Algorithm for Significantly Improved Image-Domain Material Decomposition in Dual Energy CT [J]. *Medical Physics*, 2015, 42(6):3569.
- [16] Dangguo Shao, Ting Zhou, Fan Liu. Ultrasound speckle reduction based on fractional order differentiation [J]. *Journal of Medical Ultrasonics*, 2016, 44(3):1-11.
- [17] Daniel Haak, Charles-E Page, Thomas M Deserno. A Survey of DICOM Viewer Software to Integrate Clinical Research and Medical Imaging [J]. *Journal of Digital Imaging*, 2015, 29(2):1-10.
- [18] Felix Fischer, M. Alper Selver, Sinem Gezer. Systematic Parameterization, Storage, and Representation of Volumetric DICOM Data [J]. *Journal of Medical & Biological Engineering*, 2015, 35(6):709-723.
- [19] T Kimpe, J Rostang, G Van Hoey. WE-D-204-04: Color Standard Display Function (CSDF): A Proposed Extension of DICOM GSDF [J]. *Medical Physics*, 2015, 42(6):3670.
- [20] Bing-jin Liang, Yue-yin Zhang, Yan-jun Lin. Study on the technology of medical image reading based on JPEG2000 [J]. *Automatic Control & Computer Sciences*, 2016, 50(4):278-284.
- [21] Padmapriya Praveenkumar, P. Catherine Priya, J. Avila. Tamper Proofing Identification and Authenticated DICOM Image Transmission Using Wireless Channels and CR Network [J]. *Wireless Personal Communications*, 2017, 97(4):5573-5595.
- [22] Reiji KATAYAMA. Series: Practical Evaluation of Clinical Image Quality (3): Subjective Evaluation of Image Quality in Digital Radiography Systems [J]. *Igaku Butsuri*, 2016, 36(2):113-T

- [23] Moser, S Stefanowicz, B Rhein. SU-F-J-21: *Clinical Evaluation of Surface Scanning Systems in Different Treatment Locations [J]. Medical Physics, 2016, 43(6):3410-3410.120.*
- [24] M Schmidt, N Knutson, J Herrington. SU-F-T-262: *Commissioning Varian Portal Dosimetry for EPID-Based Patient Specific QA in a Non-Aria Environment [J]. Medical Physics, 2016, 43(6):3522-3523.*
- [25] Y Altundal, D Pokhrel, H Jiang. SU-F-I-02: *Comparative Analysis and Constancy Check of Image Quality Parameters for Three Linear Accelerators Per TG 142 Protocol [J]. Medical Physics, 2016, 43(6):3386-3387.*